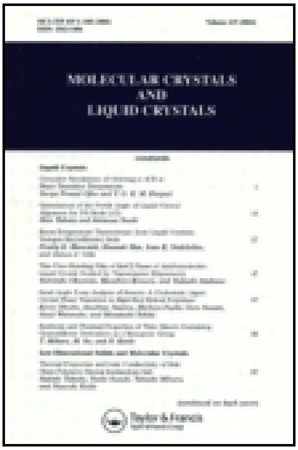

Molecular Crystals and Liquid Crystals Science and Technology. Section A. Molecular Crystals and Liquid Crystals

Publication details, including instructions for authors and subscription information:
http://www.tandfonline.com/loi/gmcl19

# Dielectric Anisotropy and AC Conductivity of Bicomponent Mixtures of Liquid Crystals Cholesteryl Pelargonate and Nonyloxybenzoic Acid

S. L. Srivastava [a] & Ravindra Dhar [a]

[a] Physics Department, University of Allahabad, Allahabad, 211002, India

Version of record first published: 04 Oct 2006

To cite this article: S. L. Srivastava & Ravindra Dhar (1998): Dielectric Anisotropy and AC Conductivity of Bicomponent Mixtures of Liquid Crystals Cholesteryl Pelargonate and Nonyloxybenzoic Acid, Molecular Crystals and Liquid Crystals Science and Technology. Section A. Molecular Crystals and Liquid Crystals, 317:1, 23-36

To link to this article: http://dx.doi.org/10.1080/10587259808047103

*Mol. Cryst. Liq. Cryst.*, Vol. 317, pp. 23-36
Reprints available directly from the publisher
Photocopying permitted by license only

# Dielectric Anisotropy and AC Conductivity of Bicomponent Mixtures of Liquid Crystals Cholesteryl Pelargonate and Nonyloxybenzoic Acid

S. L. SRIVASTAVA* and RAVINDRA DHAR

*Physics Department, University of Allahabad, Allahabad – 211 002, India*

*(Received 20 December 1996; In final form 19 August 1997)*

Dielectric constant ($\varepsilon'$) and electrical conductivity ($\sigma$) of the binary mixtures of cholesteryl pelargonate (ChP) and nonyloxybenzoic acid (NOBA) of different concentrations have been measured in the frequency range of 100 Hz to 10 MHz from room temperature to 150°C both in planar and homeotropic alignments. These mixtures do not show the dielectric dispersion upto 10 MHz. Dielectric constants parallel and perpendicular to helical axes ($\varepsilon'_{\parallel}$ and $\varepsilon'_{\perp}$) and the dielectric anisotropy ($\Delta\varepsilon' = \varepsilon'_{\parallel} - \varepsilon'_{\perp}$) have been determined in different mesophases. Dielectric anisotropy ($\Delta\varepsilon'$) of the mixtures changes sign from negative to a positive value for NOBA concentrations above 75 mole %. From the measured frequency dependent conductivity $\sigma(f)$, d.c. conductivity $\sigma(\text{dc})$ has been obtained using the universal power law equation. Activation energy ($W_a$) of the d.c. conduction process has been determined in different mesophases.

*Keywords:* Liquid crystal mixture; cholesteryl pelargonate; nonyloxybenzoic acid; dielectric anisotropy; conductivity

## INTRODUCTION

Liquid crystal mixtures are of considerable interest both because of their technological importance [1] and also for the study of molecular interactions responsible for the mesophases [2]. The binary systems of cholesterics (N*) and nematics (N) are characterized by the induction of extra helical twisting [3], arising due to interactions between molecules of different groups [4, 5]. The thermodynamic properties of a cholesteric-nematic binary system of

---

*Corresponding author.

cholesteryl pelargonate (ChP) and nonyloxybenzoic acid (NOBA) have been recently reported by us [6] confirming the earlier reported induced SmA* phase by Lavrentovich *et al.* [7–8]. The phase diagram has been drawn by us [6] considering the thermodynamic properties and optical texture which shows that smectic A (SmA) phase is stabilized and becomes enantiotropic on addition of small concentrations of NOBA and SmA* phase is induced on adding 20 to 50 mole % of NOBA. SmC phase of NOBA gets suppressed on adding 10 mole % of ChP. A wide range cholesteric (N*) phase is observed for 10 to 40 mole % of ChP. The system is eutectic at 28±2 mole % of NOBA. In the present paper we report the dielectric properties of ChP-NOBA binary system. For the dielectric study we have chosen the following four mixtures representing different mesophases alongwith pure ChP and NOBA. Extrapolated transition temperatures at the scanning rate of 0°C/min obtained from DSC [6, 9] give the following transition schemes for the systems studied here

(i) ChP: K(78.2)N*(89.7)I(89.8)N*(74.0)SmA(overnight cooling)K,

(ii) NOBA: K(91.2)SmC(115.8)N(141.8)I(141.9)N(115.8)SmC(90.5) K′(67.3)K, where K and K′ represent the crystal and mixed crystal phases respectively and I represents isotropic liquid phase.

(iii) Mixture 1: (NOBA 18.18 mole %) K(69.8)K′(73.2)SmA(79.9)SmA*(81.1)N*(92.3)I(92.5)N*(82.1) SmA*(80.0)SmA(over night cooling)K

(iv) Mixture 2: (eutectic composition, NOBA 33.33 mole %) K(69.9)SmA(80.7)SmA*(81.6)N*(93.8)I(94.2)N*(83.8)SmA*(81.0) SmA(overnight cooling)K

(v) Mixture 3: (NOBA 74.92 mole %) K(68.9)K′(85.7)N*(121.6)I(122.0)N*(71.5)K′(60.2)K

(vi) Mixture 4: (NOBA 92.55 mole %) K(68.7)K′(90.0)SmC(94.1)N*(136.0)I(136.2)N*(93.4)SmC(83.0) K′(61.9)K

## EXPERIMENTAL TECHNIQUES

The mixtures have been prepared from weighed out portions of the pure components of ChP and NOBA. These mixtures were homogenized before taking the measurements by heating to a temperature several degrees above the transition to the isotropic phase, stirring well and finally cooling.

Dielectric constant ($\varepsilon'$) and conductivity ($\sigma$) of these mixtures have been measured on a Hewlett-Packard impedance analyzer model HP-4194A equipped with a data acquisition system HP-300 [9]. Electrical cells in the form of a parallel plate capacitor were prepared by indium tin oxide (ITO) coated glass plates using 20 μm thick spacers. Planar alignment of the molecules has been achieved by coating the conducting surfaces of the glass plates with polyamide nylon and then rubbing them unidirectionally by cotton. For the homeotropic alignment, the electrode surfaces were coated with lecithin. After filling the samples in the isotropic phase, cells have been cooled very slowly (~0.2°C/min) in the first thermal cycle in order to get best possible alignment. In the second thermal cycle, samples are slowly heated to isotropic phase and then data are acquired while cooling. The computer programme for the measurement of capacitance ($C$) in parallel to conductance ($G$) has been developed to run it at 401 points in swept log scale. Frequency ($f$) of the measurement have been limited to 10 MHz because leads of the capacitor cell show inductive effect above 1 MHz [10].

Maximum uncertainty in the measurement of $\varepsilon'$ is about 20% at 100 Hz which decreases to 2% to 10 kHz and 1% at 1 MHz. Maximum uncertainty in the measurement of $\sigma$ is about 100% at 100 Hz which decreases to 6% for 10 kHz to 1 MHz. Sample temperature was controlled to an accuracy of ±0.05°C by a temperature controller of Julabo model F-20 HC.

## RESULTS AND DISCUSSION

### Pure ChP

Dielectric properties of cholesteryl pelargonate (ChP) has already been reported by us [11]. Dielectric anisotropy ($\Delta\varepsilon' = \varepsilon'_{\parallel} - \varepsilon'_{\perp}$) of ChP is negative and $|\Delta\varepsilon'|$ increases as temperature decreases. In both planar and homeotropic alignments ChP molecules do not show dispersion upto 10 MHz. D.C. conductivity $\sigma$(dc) of ChP lies in the range of $10^{-9}-10^{-10}$ S-m$^{-1}$ in I phase. In the mesophases it becomes less than $10^{-10}$ S-m$^{-1}$ and is beyond the measuremental limit of the impedance analyzer. Activation energies of d.c. conductivities ($W_a$) for I phase of ChP is $28 \pm 9$ kcal/mole.

### Pure NOBA

Dielectric constant ($\varepsilon'$) and loss ($\varepsilon''$) of NOBA as a function of frequency have been measured at different temperatures between crystal to isotropic liquid phase. Dielectric constants parallel and perpendicular to helical axes ($\varepsilon'_{\parallel}$ and $\varepsilon'_{\perp}$) are constant with frequency upto 1 MHz. Variations of $\varepsilon'_{\parallel}$ and

$\varepsilon'_\perp$ at 100 kHz with temperature for the second cooling cycle of NOBA are shown in Figure 1 where vertical bars show maximum uncertainty in the measurement of $\varepsilon'$. At I-N transition temperature ($T_{\mathrm{IN}}$), both $\varepsilon'_\perp$ and $\varepsilon'_\parallel$ are lower than its isotropic value ($\varepsilon'_{\mathrm{I}}$) (see Fig. 1) and hence $\varepsilon'_{av}[= (1/3)(\varepsilon'_\parallel + 2\varepsilon'_\perp)]$ of the nematic phase is less than $\varepsilon'_{\mathrm{I}}$. The dielectric loss ($\varepsilon'' = \sigma/\varepsilon_0\omega$) follows the same behaviour.

Anisotropies of dielectric constant and loss ($\Delta\varepsilon'$ and $\Delta\varepsilon''$) of NOBA are positive in N phase with a maximum value of $\Delta\varepsilon' = +0.05$ at 130°C, which becomes negative in SmC phase. $\Delta\varepsilon'$ of NOBA is almost of the same magnitude as reported by other workers [12–14]. The sign reversal in dielectric anisotropy with decrease in the temperature has been observed in other systems also [15–18]. With increase in the number of thermal cycles of NOBA, $\Delta\varepsilon'$ $(= \varepsilon'_\parallel - \varepsilon'_\perp)$ decreases and becomes negative in N phase also.

Dielectric data of NOBA can be explained by assuming three types of clusters in the sample: monomers with the single molecules, cyclic dimers of two molecules with two hydrogen bonds between COOH groups of NOBA and open dimers of two molecules with one broken hydrogen bond [19]. For a cyclic dimer net dipole moment ($\mu$) becomes almost zero [12] due to antiparallel combination of molecules. However for an open dimer (one hydrogen bond broken) there is a possibility of increase in transverse

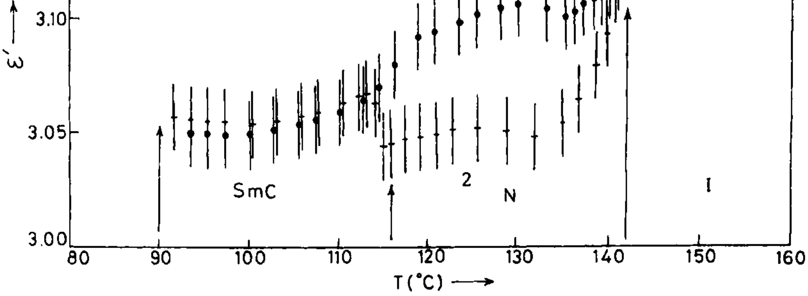

FIGURE 1 Variation of dielectric constants $\varepsilon'_\parallel$ and $\varepsilon'_\perp$ with temperature (°C) at 100 kHz for cooling cycle of NOBA. Curve 1 for $\varepsilon'_\parallel$ and 2 for $\varepsilon'_\perp$. Upward vertical arrows show transition temperatures as obtained from DSC.

component of dipole moment ($\mu_\perp$) and decrease in longitudinal component of dipole moment ($\mu_\parallel$). For the monomer of NOBA, $\mu_\parallel < \mu_\perp$, because of COOH group where $\mu$ makes an angle of 74° with C—C bond axis [20]. The population of the monomers in I phase may be assumed to be the maximum. At I-N transition, a rapid combination of two monomers into a cyclic dimer may increase the population of cyclic dimers [21], resulting in decrease of both $\varepsilon'_\parallel$ and $\varepsilon'_\perp$ (see Fig. 1). The magnitude of the change may depend upon the ratio of populations of dimers in N phase to that in I phase. For the monomers of NOBA, $\Delta\varepsilon'$ is negative, but a positive value of $\Delta\varepsilon'$ in N phase may be the consequence of parallel dipole-dipole correlation between the neighbouring dimers. However in SmC phase an antiparallel dipole-dipole correlation is expected [18, 22, 23] which may decrease $\varepsilon'_\parallel$ and hence $\Delta\varepsilon'$.

Conductivity data follow the universal power law [24]

$$\sigma(f) = \sigma(\mathrm{dc}) + A_0 f^m \tag{1}$$

where $m = 2-\alpha$, $\alpha$ is the symmetric distribution parameter. The value of $m$ for the mesophases of NOBA and ChP lies in the range of 1.6 to 1.9 indicating that conductivity is mainly due to the dipolar orientations. Contribution of the frequency dependent term at lower frequencies (< 1 kHz) is very small and the conductivity is mainly due to $\sigma$(dc). The plot of $\log(\sigma(f))$ against $\log(f)$ gives $\sigma$(dc) at different temperatures which are of the order of $10^{-6}$ S-m$^{-1}$ in I phase of NOBA and decreases with decrease in the temperature. In the crystal phase $\sigma$(dc) is of the order of $10^{-9}$–$10^{-10}$ S-m$^{-1}$. Chou and Carr [21] have measured $\sigma$(dc) of NOBA to be of the order of $10^{-7}$ S-m$^{-1}$. Arrhenius plots of $\sigma$(dc) are given in Figure 2 for both planar and homeotropic aligned samples where vertical bars show maximum uncertainty in the determination of $\sigma$(dc). Figure 2 shows that for mesophases $\sigma(\mathrm{dc})_\parallel < \sigma(\mathrm{dc})_\perp$ at all temperatures which agrees to the observations of the other workers [12, 13]. Using the Arrhenius equation

$$\sigma(\mathrm{dc}) = \sigma_0 \exp(-W_a/kT) \tag{2}$$

activation energies of dc conductivities ($W_a$) have been obtained for I, N and SmC phases. In the homeotropic alignment of the sample, $W_a$ for N and SmC phases are 38 and 16 kcal/mole respectively, while in the planar alignment, $W_a$ are 8 and 24 kcal/mole respectively for N and SmC phases. For the isotropic phase $W_a$ is 3 kcal/mole in the vicinity of $T_{\mathrm{IN}}$, while away from $T_{\mathrm{IN}}$ it is about 9 kcal/mole manifesting a large pretransitional effect.

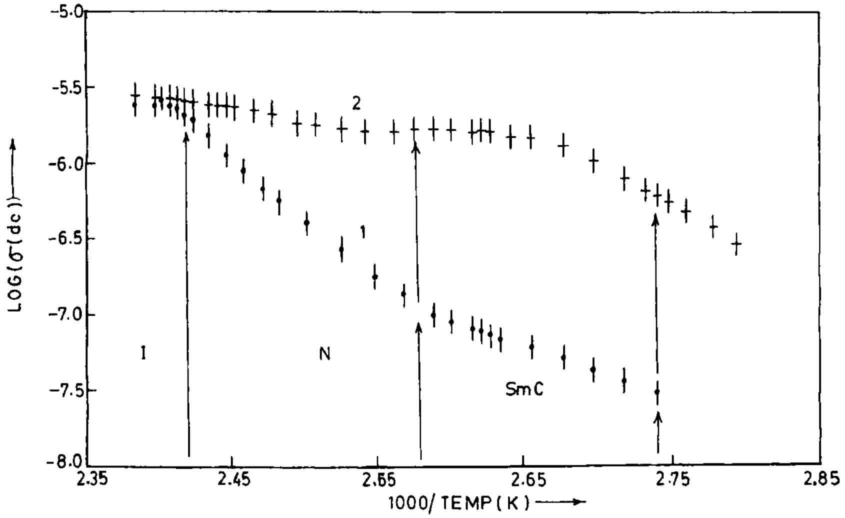

FIGURE 2 Variation of log of d.c. conductivity with 1000/$T$(K) for cooling cycle of NOBA. Curve 1 for homeotropic alignment and 2 for planar alignment. Upward vertical arrows show transition temperatures as obtained from DSC.

## MIXTURES OF CHP AND NOBA

Variations of $\varepsilon'_{\parallel}$ and $\varepsilon'_{\perp}$ at 100 kHz with temperature (in °C) for the second cooling cycle are shown in Figures 3–6 for the four mixtures of ChP and NOBA where vertical bars represent maximum uncertainty in the measurement of $\varepsilon'$. In I phase as temperature decreases, dielectric constant ($\varepsilon'_{\mathrm{I}}$) increases. Below the isotropic to cholesteric transition temperature ($T_{\mathrm{IN}^*}$) molecules start aligning. For the mixture 2 (eutectic composition, NOBA 33.33 mole %), even in N* phase $\varepsilon'_{\parallel} \cong \varepsilon'_{\perp}$ and anisotropy in $\varepsilon'$ is observed only when N* phase ends. In mixture 3 (NOBA 74.92 mole %), alignment of the molecules starts 2–3°C above $T_{\mathrm{IN}^*}$, showing strong pretransitional effects.

At the transition temperatures, $\varepsilon'_{\parallel}$ and $\varepsilon'_{\perp}$ show discontinuities. $d\varepsilon'/dT$ shows peaks (see Fig. 7) at the transition temperatures, which are in agreement with DSC experiment [6]. SmA-K transition temperature of mixtures 1 and 2 have been observed at 47 ± 3 and 51 ± 1°C by the dielectric measurements after cooling them for 2–4 hours, which have not been observed by the DSC experiment. For mixtures 3 and 4, N*–K′ and SmC–K′ transition temperatures are observed at 77.2 ± 1 and 88.5 ± 1°C respectively which are slightly higher than those observed from DSC experiment.

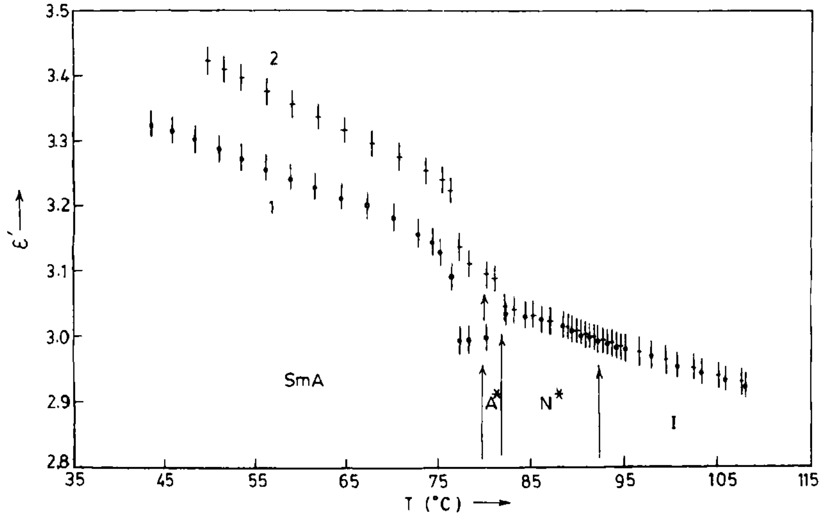

FIGURE 3 Variation of dielectric constants $\varepsilon'_{\parallel}$ and $\varepsilon'_{\perp}$ at 100 kHz with temperature (°C) for cooling cycle of the mixture 1 of NOBA and ChP (NOBA 18.18 mole %). Curve 1 for $\varepsilon'_{\parallel}$ and 2 for $\varepsilon'_{\perp}$. Upward vertical arrows show transition temperatures as obtained from DSC.

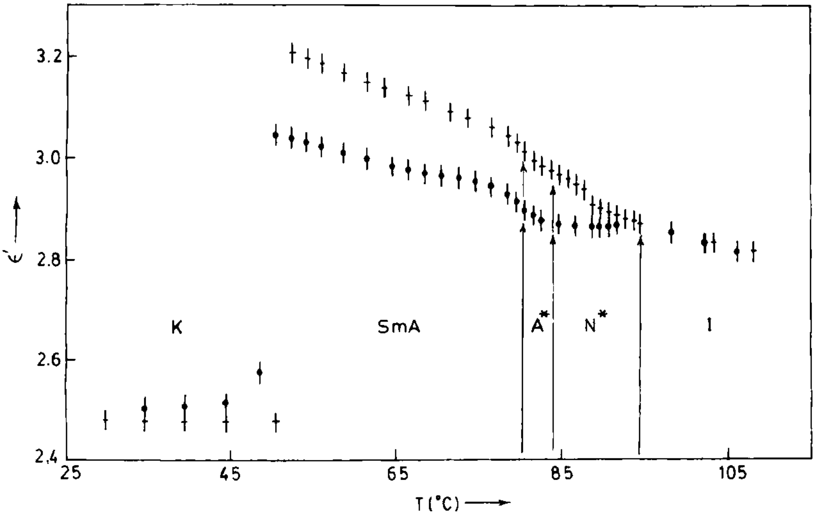

FIGURE 4 Variation of dielectric constants $\varepsilon'_{\parallel}$ and $\varepsilon'_{\perp}$ at 100 kHz with temperature (°C) for cooling cycle of the mixture 2 of NOBA and ChP (NOBA 33.33 mole %). Curve 1 for $\varepsilon'_{\parallel}$ and 2 for $\varepsilon'_{\perp}$. Upward vertical arrows show transition temperatures as obtained from DSC.

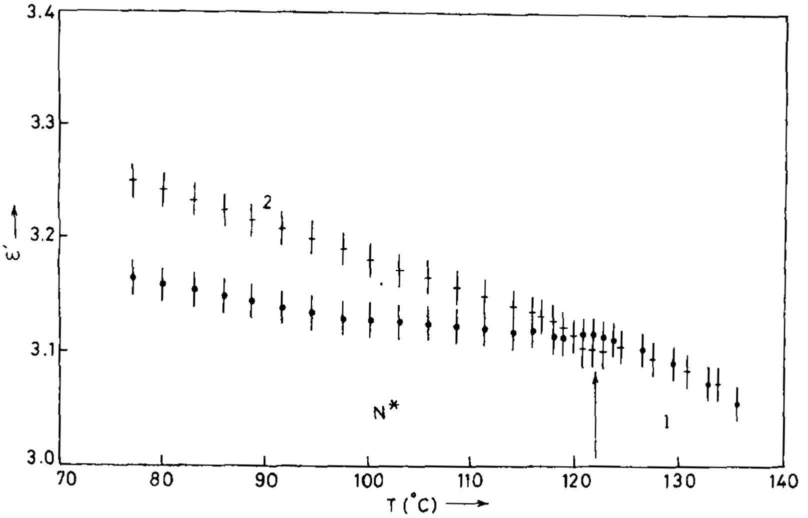

FIGURE 5 Variation of dielectric constants $\varepsilon'_{\parallel}$ and $\varepsilon'_{\perp}$ at 100 kHz with temperature (°C) for cooling cycle of the mixture 3 of NOBA and ChP (NOBA 74.92 mole %). Curve 1 for $\varepsilon'_{\parallel}$ and 2 for $\varepsilon'_{\perp}$. Upward vertical arrows show transition temperatures as obtained from DSC.

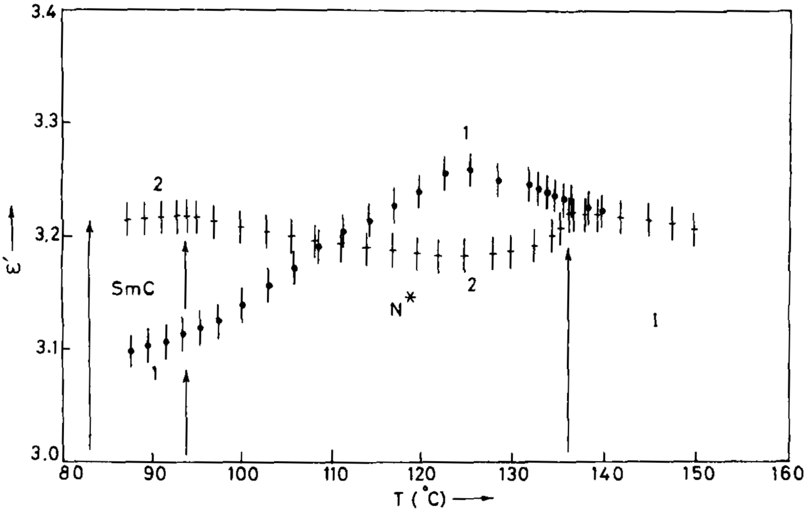

FIGURE 6 Variation of dielectric constants $\varepsilon'_{\parallel}$ and $\varepsilon'_{\perp}$ at 100 kHz with temperature (°C) for cooling cycle of the mixture 4 of NOBA and ChP (NOBA 92.55 mole %). Curve 1 for $\varepsilon'_{\parallel}$ and 2 for $\varepsilon'_{\perp}$. Upward vertical arrows show transition temperatures as obtained from DSC.

Dielectric anisotropy ($\Delta\varepsilon'$) for second thermal cycle of pure components and mixtures has been plotted against the reduced temperature ($T_{\text{red}} = T/T_{\text{IN}}$) in Figure 8. At $T_{\text{red}} = 1$, dielectric constant in the isotropic phase ($\varepsilon'_{\text{I}}$) is

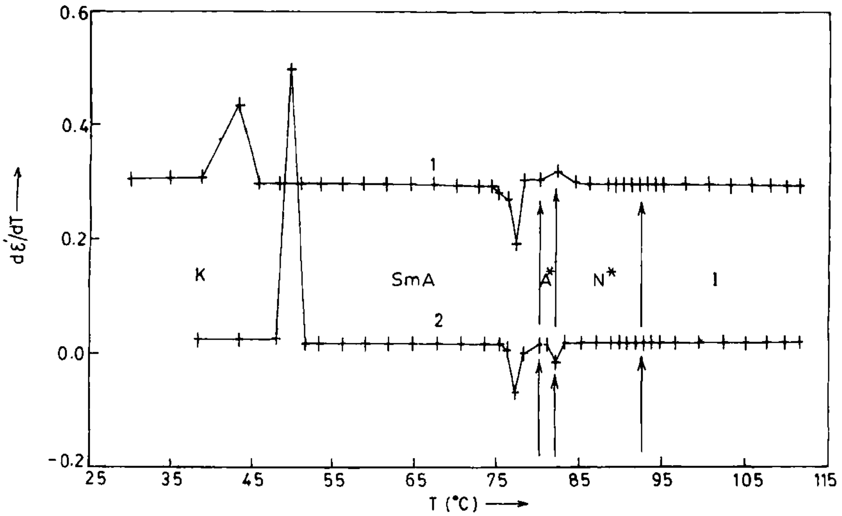

FIGURE 7 Variation of $d\varepsilon'/dT$ at 100 kHz with temperature (°C) for cooling cycle of the mixture 2 of NOBA and ChP (NOBA 33.33 mole %). Curve 1 for $d\varepsilon'/dT$ (shifted by 0.3) and curve 2 for $d\varepsilon'_{\perp}/dT$. Upward vertical arrows show transition temperatures as obtained from DSC.

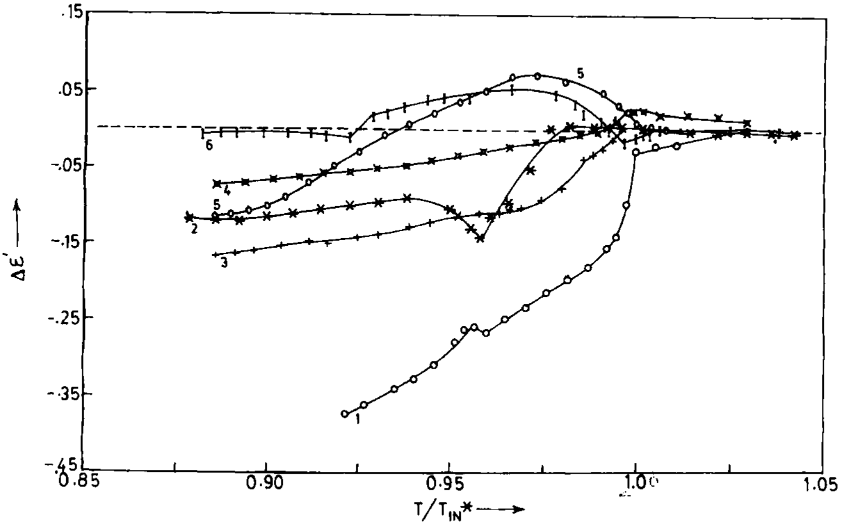

FIGURE 8 Variation of dielectric anisotropy ($\Delta\varepsilon'$) with $T/T_{\mathrm{IN}^*}$. Curve 1 for pure ChP, curve 2 for mixture 1 (NOBA 18.18 mole %), curve 3 for mixture 2 (NOBA 33.33 mole %), curve 4 for mixture 3 (NOBA 74.92 mole %), curve 5 for mixture 4 (NOBA 92.55 mole %) and curve 6 for pure NOBA.

almost equal to the average value ($\varepsilon'_{av}$) of N* phase $[\frac{1}{3}(\varepsilon'_{\parallel}+2\varepsilon'_{\perp})_{N^*}]$ for all the mixtures studied here. For mixtures 1 and 2, $\Delta\varepsilon'$ is negative in all the mesophases. In SmA* phase of the mixture 1, $\Delta\varepsilon'$ decreases as temperature decreases and shows a minimum at SmA*-SmA transition temperature ($T_{A^*A}$) ($\Delta\varepsilon' = -0.15$, see Figs. 3 and 8). While going from SmA* to SmA phase $\Delta\varepsilon'$ increases and becomes almost constant with temperature in the stabilized SmA phase. In SmA phase $\Delta\varepsilon'$ is still negative and it is −0.12 just before the crystallization occurs at 47±3 °C. This value of $|\Delta\varepsilon'|$ is less than that of pure ChP (~0.40). For mixture 2 also, $\Delta\varepsilon'$ decreases with temperature in SmA* phase whereas it is a constant in SmA phase. For mixture 2, $\Delta\varepsilon'$ is not a minimum at $T_{A^*A}$ as observed in mixture 1.

Mixtures 3 (74.92 mole % of NOBA) and 4 (92.55 mole % of NOBA), show a tendency of positive dielectric anisotropy in N* phase when these are cooled from I phase (see Fig. 8). With further decrease in the temperature of N* phase, $\varepsilon'_{\parallel}$ and $\varepsilon'_{\perp}$ show cross overs (see Figs. 5 and 6) and $\Delta\varepsilon'$ becomes negative. For mixture 4 the cross over temperature is 109°C which is lower than that of mixture 3 (120°C). For these two mixtures, $\varepsilon''_{\parallel}$ and $\varepsilon''_{\perp}$ also show cross overs with lowering in temperature.

ChP has a negative dielectric anisotropy in all the mesophases, but NOBA has a small positive dielectric anisotropy in the nematic phase and a very small negative anisotropy in SmC phase (see Fig. 8). For mixtures dielectric anisotropy ($\Delta\varepsilon'$) of mesophases and the dielectric constant in the isotropic phase ($\varepsilon'_I$) lie between those of ChP and NOBA (see Figs. 8 and 9). It seems that upto the eutectic composition dielectric properties of the mixtures are governed by ChP. Mixtures 3 and 4 show a positive $\Delta\varepsilon'$ just below $T_{red} = 1$, which shows reversal only at considerably lower value of $T_{red}$. The temperature range of positive anisotropy as well as its magnitude increase with the concentration of NOBA above the eutectic composition. The dielectric behaviour of mixtures 3 and 4 are thus similar to that of NOBA. At the eutectic composition (33.33 mole % of NOBA) both $\Delta\varepsilon'$ and $\varepsilon'$ show dips (see Figs. 8 and 9). It is remarkable that transition temperatures ($T_P$) of all the mesophases, transition enthalpy (ΔH) and transition entropy (ΔS) of N*-I transition also show dip for eutectic composition of ChP-NOBA mixture [6]. Kleinhans *et al.* [25] have observed a similar dip in the plot of $dT/dP$ with mole fraction of 6OCB in 8OCB. In the mixture of cholesteryl chloride and cholesteryl alkanoate $|\Delta\varepsilon'|$ decreases as the chain length of alkanoate increases [26]. In ChP-NOBA system also as NOBA molecules are introduced into ChP matrix, average molecular length increases [6] hence $|\Delta\varepsilon'|$ decreases.

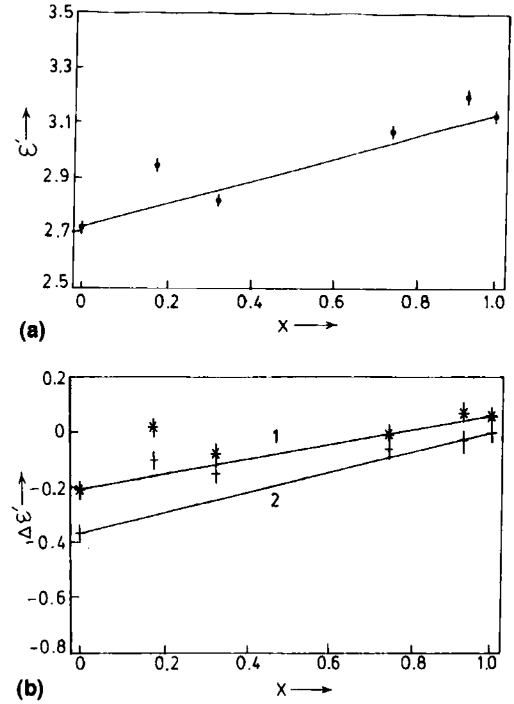

FIGURE 9 (a) Variation of dielectric constant of the isotropic phase ($\varepsilon'_{\mathrm{I}}$) with mole fraction of NOBA ($x$) at $T_{\mathrm{red}} = 1.03$ (b) Variation of dielectric anisotropy ($\Delta\varepsilon'$) with mole fraction of NOBA ($x$), ($*$) represents $\Delta\varepsilon'$ at $T_{\mathrm{red}} = 0.98$ and ($+$) represents $\Delta\varepsilon'$ at $T_{\mathrm{red}} = 0.925$.

Change in sign of $\Delta\varepsilon'$ has been observed in mixtures also [17, 27, 28]. Sign reversal of $\Delta\varepsilon'$ with temperature in the mixtures 3 and 4 can not be explained on the basis of parallel correlation of transverse component of the dipole moment ($\mu_{\perp}$) and antiparallel correlation of longitudinal component ($\mu_{\parallel}$) within the smectic layers [15] because there is no smectic phase in the mixture 3. Chandrasekhar *et al.* [17] explain the reversal of dielectric anisotropy data of the mixture of *p*-azoxyanisole (PAA) and 4'-*n*-methoxybenzylidene (5CT) on the basis of Maier and Meier theory [29] according to which if polarizability ($\Delta\alpha$) and permanent dipolar ($\mu^2$) contributions are nearly balanced, then there can be a reversal of $\Delta\varepsilon'$ on lowering the temperature. In the mixture of PAA and 5CT as concentration of 5CT increases the crossover temperature decreases. Reversal of $\Delta\varepsilon'$ in PAA-MBPAA (4-*n*-methoxybenzylidene-4'-phenylazoaniline) mixture which has only N phase has been explained on this basis [17]. For ChP-NOBA system also dipolar contribution dominates for mixtures 1 and 2 and

$\Delta\varepsilon'$ is negative at all the temperatures as that in ChP. However due to a small positive anisotropy of NOBA, polarizability and dipolar contributions in Maier and Meier equation may nearly be equal for mixtures 3 and 4 and reversal in $\Delta\varepsilon'$ may occur on decreasing the temperature.

Dielectric constant of the isotropic phase ($\varepsilon'_I$) and dielectric anisotropy ($\Delta\varepsilon'$) of the mixtures in different mesophases are found to be nonadditive as shown in Figure 9 where vertical bars show uncertainties in the determination of $\varepsilon'_I$ and $\Delta\varepsilon'$. According to Kresse [14] since the factors of the reaction field in Maier and Meier equation for $\varepsilon'$ and $\Delta\varepsilon'$ are not linear with $x$, hence a simple additivity of $\varepsilon'_I$ and $\Delta\varepsilon'$ for rod like molecules should not hold.

Electrical conductivity ($\sigma$) of these mixtures follow the universal power law given by Eq. (1) from which d.c. conductivity ($\sigma$(dc)) have been obtained at different temperatures from $\sigma(f)$ vs $\log(f)$ plots (see Fig. 10). For all the mixtures d.c. conductivity along the long axes of the molecules ($\sigma(\mathrm{dc})_{\parallel}$) is larger than in direction perpendicular to the long axes ($\sigma(\mathrm{dc})_{\perp}$) excluding the case of eutectic mixture 2 for which $\sigma(\mathrm{dc})_{\parallel} < \sigma(\mathrm{dc})_{\perp}$. Activation energy ($W_a$) of $\sigma$(dc) for different mesophases of these mixtures have been estimated by the Arrhenius Eq. (2) and they are listed in Table I from which it has been found that the activation energies for dc conduction along the long axes of

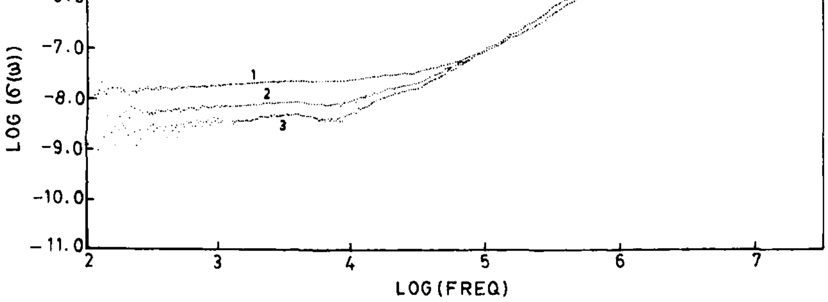

FIGURE 10 Variation of log of conductivity with log of frequency for the mixture 2 of NOBA and ChP (NOBA 33.33 mole %) at different temperatures in I, N* and SmA* phases. Curve 1 at 108°C (I phase), curve 2 at 85 °C (N* phase) and curve 3 at 78°C (SmA* phase).

TABLE I Activation energy of d.c. conductivities ($W_a$ in kcal/mole) for different mesophases of the mixtures in homeotropic ($H$) and planar ($P$) alignments

| *mole fraction* | *←I→* | *←N*→* | | *←SmC→* | | *←SmA→* | |
|---|---|---|---|---|---|---|---|
| *of NOBA (x)* | | *H* | *P* | *H* | *P* | *H* | *P* |
| 0 | 28 | – | – | – | – | – | – |
| 18.18 | 12 | 35 | 23 | – | – | 38 | 27 |
| 33.33 | 16 | 34 | 31 | – | – | 19 | 13 |
| 74.92 | 4 | 17 | 15 | – | – | – | – |
| 92.55 | 7 | 24 | 22 | 21 | 13 | – | – |
| 100 | 9 | 38 | 8 | 16 | 24 | – | – |

the molecules ($(W_a)_{\parallel}$) are larger than $(W_a)_{\perp}$ except for SmC phase of NOBA. For cholesteryl laurate, cholesteryl caprilate and their mixtures also it has been observed that $(W_a)_{\parallel} > (W_a)_{\perp}$ in the smectic phases and the conduction of the charge carriers is assigned to the hopping mechanism [28].

## Acknowledgements

We express our thanks to Dr. V. K. Agrawal and Ms. Arunima Mukherjee for their help during the progress of this work. We also thank University Grants Commission, New Delhi for the financial assistance.

## References

[1] Liquid Crystals: Applications and Uses, Vol. I, II and III, Ed. B. Bahadur, World Scientific, Singapore (1995).

[2] E. P. Sokolova and A. Y. Vlasov, *Liq. Cryst.*, **8**, 47 (1990).

[3] N. L. Kramarenko, N. M. Shkabara, L. G. Derkach and M. V. Loseva, *Sov. Phys. Crystallogr.*, **35**, 462 (1990).

[4] L. N. Lisetski, V. D. Panikarskaya, T. P. Antonyan and L. A. Batrachenko, *Sov. Phys. Crystallogr.*, **36**, 868 (1991).

[5] L. N. Lisetski, L. A. Batrachenko and V. D. Panikarskaya, *Mol. Cryst. Liq. Cryst.*, **215**, 287 (1992).

[6] S. L. Srivastava, R. Dhar and A. Mukherjee, *Mol. Cryst. Liq. Cryst.*, **287**, 139 (1996).

[7] O. D. Lavrentovich and Y. A. Nastishin, *Ukr. Fiz. Zhurn.*, **35**, 221 (1990).

[8] O. D. Lavrentovich, Y. A. Nastishin, V. I. Kulishov, Y. S. Narkevich, A. S. Tolochko and S. V. Shiyanovskii, *Europhysics Letters*, **13**, 313 (1990).

[9] S. L. Srivastava, R. Dhar and M. V. Kurik, *Mol. Mat.*, **2**, 261 (1993).

[10] S. L. Srivastava, *Proc. Nat. Acad. Sci.* (India), **63**, 311, (1993).

[11] S. L. Srivastava and R. Dhar, *Rad. Phys. Chem.*, **47**, 287 (1996).

[12] E. F. Carr, *Pramana Suppl.*, **1**, 263 (1975).

[13] L. S. Chou and E. F. Carr, *Proc. ACS Symp.*, on Ordered Fluid and Liquid Crystals, Chicago (Aug. 26–31, 1973), Plenum Press, New York.

[14] H. Kresse, *Adv. Liq. Cryst.*, **6**, 109 (1983), Academic Press, Inc New York.

[15] W. H. de Jeu, T. W. Lathouwers and P. Bordewijk, *Phys. Rev. Lett.*, **32**, 40 (1974).

[16] L. Benguigui, *J de Physique*, **40**, 705 (1979).

[17] S. Chandrasekhar and B. R. Ratna, *Mol. Cryst. Liq Cryst.*, **82**, 193 (1982).

[18] A. J. Martin, G. Meier and A. Saupe, *Symp. of the Faraday Soc.*, **5119** (1971).

[19] B. Deloche and B. Cabane, *Mol. Cryst. Liq. Cryst.*, **19**, 25 (1972).

[20] N. E. Hill, W. E. Vaughan, A. H. Price and M. Davies, Dielectric Properties and Molecular Behaviour, Van Nostran Reinhold Co. (1969), p. 246.

[21] L. S. Chou and E. F. Carr, *Phys. Rev. A*, **7**, 1639 (1973).

[22] J. W. Goodby, *Mol. Cryst. Liq. Cryst.*, **75**, 179 (1981).

[23] D. Coates, *Liq. Cryst.*, **2**, 63 (1987).

[24] A. K. Johnscher, *Nature*, **269**, 673 (1977).

[25] H. D. Kleinhans, R. Shashidhar and G. M. Schneider, *Mol. Cryst. Liq. Cryst.* (letters), **82**, 19 (1982).

[26] C. K. S. Nair and K. V. Ramanaiah, *Mol. Cryst. Liq. Cryst.*, **103**, 271 (1983).

[27] B. S. Srikanta and N. V. Madhusudana, *Mol. Cryst. Liq. Cryst.*, **103**, 111 (1983).

[28] M. Honciuc, C. Motoc and O. Savin, *Mol. Cryst. Liq. Cryst.*, **95**, 339 (1983).

[29] W. Maier and G. Meier, *Z. Naturforsch*, **16A**, 262 (1961).